Research Article

Eroded topography in Proterozoic Basement: the case of Capiá river watershed, Semi-arid Northeastern Brazil

Topografia erodida em Escudo Proterozoico: o caso da bacia hidrográfica do rio Capiá, Semiárido do Nordeste do Brasil

Genisson Panta [1], João Paulo da Hora Nascimento [2] Kleython de Araújo Monteiro [3]

[1] Universidade Federal de Alagoas, IGDEMA, Maceió, Brasil. genissongeo@gmail.com
ORCID: http://orcid.org/0000-0002-6745-7772

[2] Universidade Federal de Pernambuco, DCG, Recife, Brasil. joao.hora@ufpe.br
ORCID: http://orcid.org/0000-0003-4111-0524

[3] Universidade Federal de Alagoas, IGDEMA, Maceió, Brasil. kleython.monteiro@igdema.ufal.br
ORCID: http://orcid.org/0000-0003-4829-3722

Abstract: It is a consensus that the semi-arid depressions created in Atlantic Proterozoic Shield underwent intense denudational processes, especially during the Cenozoic. However, there are still no studies on quantifying and spatializing the fluvial incision for the Southern Sertaneja Depression, low course of the São Francisco river. Then, this study sought to quantify and spatialize the fluvial incision over the Proterozoic basement in the Capiá river basin through the integration of geoprocessing and geostatistical techniques (ordinary kriging), based on a Digital Elevation Model. Correlations were drawn between lithological resistance, basement structures and geomorphological aspects. More than half of the analyzed watershed mass has already been removed by denudational processes and the minimum bulk erosion per corresponding area is in contrast with other regions of the planet. The reconstitution of the topography allowed the delimitation of two large morphostructural compartments in the basin. Finally, apatite fission track data from studies already published in the study area were presented.

Keywords: Sertaneja Depression, Atlantic Shield, bedrock.

Resumo: É consenso que as depressões semiáridas elaboradas em rochas do Escudo Proterozoico Atlântico passaram por intensos processos denudacionais, especialmente durante o Cenozoico. Porém, ainda não se têm estudos de quantificação e espacialização da incisão fluvial para a Depressão Sertaneja Meridional, baixo curso do rio São Francisco. A partir disso, este estudo buscou quantificar e espacializar a incisão fluvial sobre o embasamento Proterozoico na bacia hidrográfica do rio Capiá por meio da integração de técnicas de geoprocessamento e geoestatística (krigagem ordinária), com base em um Modelo Digital de Elevação. Traçou-se correlações entre resistência litológica, estruturas do embasamento e aspectos geomorfológicos. Mais da metade da massa contida na bacia de drenagem analisada já foi removida por processos denudacionais e o volume mínimo erodido por área correspondente é contrastante com outras regiões do planeta. A reconstituição da topografia permitiu delimitar dois grandes compartimentos morfoestruturais na bacia. Finalmente, apresentou-se dados de traço de fissão em apatita de estudos já publicados na área de estudo.

Palavras-chave: Depressão Sertaneja, Escudo Atlântico, leito rochoso.

1. Introduction

Drylands cover about 1/3 of the surface of the continents (GOUDIE, 2013). Contrary to intuition, these terrains are marked by fluvial dissection, both in areas of exposed shield and covered by lithified strata (TWIDALE, 1978; GRAF, 1988). Arid and semiarid landscapes encompass a wide morphological diversity, but pediments carved in exposed shield regions are the most representative features in this context, especially in Northeastern Brazil (GODARD *et al*., 2001; CORRÊA *et al*., 2019). The amalgamation of pediments and associated morphologies, such as inselbergs and ridges, form vast planation surfaces that truncate lithologies of different degrees of strength, a testimony to the balance of the joint action of climatic, tectonic, and surface processes.

The genesis of these surfaces has been at the core of the debate in Geomorphology, and several conceptual models have been enlisted to elucidate their origin (*e.g*., ORME, 2013). The morphogenesis of these surfaces has traditionally been described as the end product of prolonged denudation cycles, in contrast to more recent studies that highlight the role of geodynamic mechanisms in the conformation of relief on a regional scale, especially when it comes to the post-rift evolution of continental margins and hinterlands (CORRÊA; MONTEIRO, 2021; SACEK et al., 2019). Likewise, the problem of planation surfaces has been put under the prism of post-orogenic landscape evolution (*e.g.,* PEULVAST; CLAUDINO-SALES, 2002; BONNET *et al.,* 2000) and lithosphere and mantle deformations (*e.g*., GUILLOCHEAU *et al*. 2018).

The relief of Northeastern Brazil was historically interpreted through cyclic theories of continental surface evolution in which episodic epeirogenic movements were associated with correlative sedimentation of peripheral basins, producing perched surfaces (MAIA; BEZERRA, 2020). On the other hand, emerging approaches are already available. Sacek *et al*. (2019), through numerical modeling, geochronological and stratigraphic data analysis, state that approximately 70% of the topography of Borborema Province can be explained by a flexural rebound and differential erosion mechanisms. The rest, still according to the authors, would be controlled by the thermal uplift process in response to the erosion of the continental lithosphere base, caused by convection at the boundary between the continental and oceanic crust. However, there is evidence for Cenozoic tectonic processes, in addition to the reported passive structural controls, exerting control on the conformation of the regional topography (*e.g*., TAVARES et al. 2014; OLIVEIRA *et al*. 2018; GURGEL *et al*. 2013)

Given these challenges, modern techniques of topography analysis, through remote sensing products, have become one of the most fruitful means of investigating structural and tectonic controls on the relief (ANDRADES FILHO; ROSSETTI, 2012). One of the applications of these data is the spatialization of eroded topography and the investigation of the tracing of river courses, one of the main modeling agents of the earth's surface. As a complementary path to essentially descriptive investigations, in areas of intraplate exposed shield, Bonnet *et al*. (2000) and Godard *et al*. (2001) highlight the role of morphometric analyses based on the Digital Elevation Model (DEM), for the investigation of fluvial dissection and tectonic reactivation along faults inherited from the basement and this has brought great contributions to the understanding of the meaning of erosion surfaces.

As highlighted, the rivers play a key role in the evolution of this type of landscape, notably the bedrock rivers. According to Tinkler and Wohl (1998), bedrock rivers are those whose rocks outcrop in the bed or banks for more than half of their extension. In this definition, substratum refers to both too hard rocks and cohesive sediment that covers the stream bed and produces a mechanical response rock-like to fluvial erosion. These reaches may be covered by a thin layer of alluvium, intensely remobilized during the rainy season. In this way, the conformation of the underlying substrate influences the flow structure and the transport of sediments. From a different perspective, Whipple (2004), based on Gilbert (1877), affirms that the physical restriction that allows bedrock rivers to occur in nature is that, in the long term, the transport capacity exceeds the bed load transportation, a condition known in the literature as detachment-limited.

Thus, this study sought to explore morphometric methods for the analysis of eroded topography in regions of the exposed Proterozoic basement through the integration between DEM, topographic maps and complementary geological mapping, in the Southern Sertaneja Depression, a set of low elevation terrains (~250 m) that surround crystalline and sedimentary plateaus in the semi-arid domain of Northeastern Brazil. Authors such as Ab'saber (1969), Mabesoone (1994) and Fernandes Lima (1992) concur that the Southern Sertaneja Depression was formed by long and intense denudational processes. However, after Jelinek *et al*. (2014), some of these assumptions have been revised, evidencing that the evolution of the relief in this region is still not fully understood. However, studies that quantify the spatial distribution of fluvial incision are still scarce in this compartment. We intend to provide quantitative measurements for the Minimum Bulk Erosion and discuss its implications, especially through the

relationships between fluvial erosion, lithological resistance and possible controls of geological structures in the lower course of the São Francisco river, at the limits of the Capiá River watershed.

2. Study Area

The watershed of the Capiá River drains 2,344 km². Its main river, as well as its tributaries, flows largely over bedrock. The Capiá covers 105 km until it flows into the São Francisco River, in the district of Entremontes, municipality of Piranhas (Figure 1). Although most of the basin is located in the Alagoas semi-arid region, a small portion of its headwaters is located in the south of Pernambuco. Its largest tributaries are the Canapi River, alongside the Carié, Alecrim, Croatá, Santa Helena, Cacimbas and Carcará creeks. The basin is crossed by federal roads BR-423 and BR-316 and state roads AL-140 and AL-220. It covers part of the Alagoas municipalities of Ouro Branco, Canapi, Inhapi, Maravilha, Poço das Trencheiras, Senador Rui Palmeira, São José da Tapera, Piranhas, Pão de Açúcar, Mata Grande and Olho D'água do Casado (FERNANDES LIMA, 1992).

The watershed of the Capiá River is composed of Proterozoic rocks that are part of the Southern or External Sector of the Borborema Province. The division of the Borborema Province is not consensual and is more geometric than evolutionary (HASUI et al., 2012). It is limited to the south by the São Francisco Craton, the Parnaíba Basin to the west and the Eastern and Equatorial Continental Margin Provinces. The Southern Sector has abundant granitic intrusions from the Brasiliano Cycle (640 to 450 Ma). The structures in this domain exhibit two general directions: NO and ENE (HASUI et al., 2012).
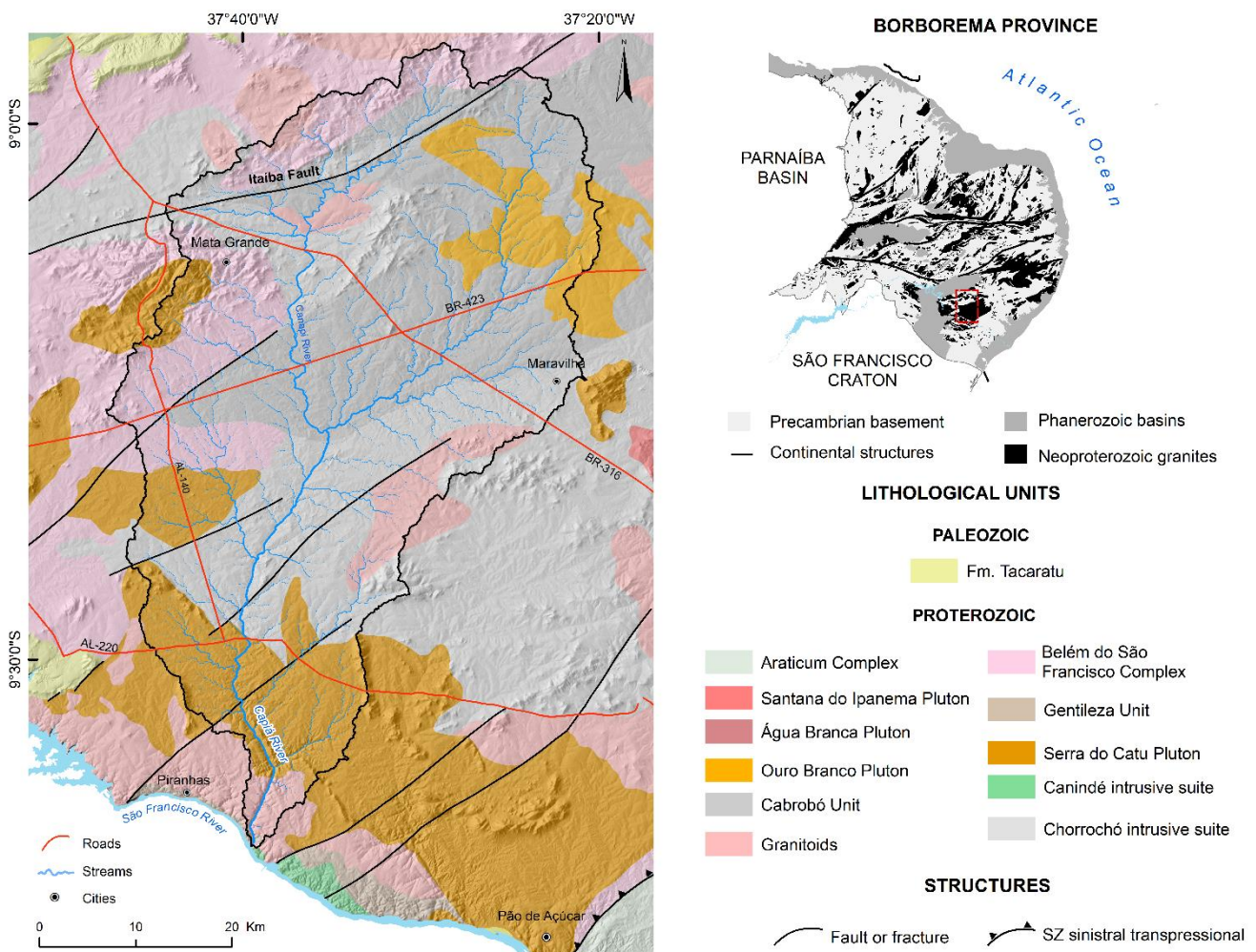

Figure 1. Location of the study area, with emphasis on the lithological units, municipal headquarters, and access roads, in addition to the drainage network and the limits of the Capiá river watershed.

According to Van Schmus *et al*. (2011), the Southern Sector of the Borborema Province is marked by the collage of crustal fragments, with ages ranging from Archean to Neoproterozoic, crossed by deep and extensive shear zones. The Borborema Province has Archean cores, but Paleoproterozoic lithologies that underlie the metavolcanic-sedimentary and metasedimentary bands that encompass granites from the Cariris Velhos (1.1 – 0.93 Ga) and Brasiliano (Pan-African) (0.75 Ga – 0.54 Ga) orogenic cycles (SANTOS; MEDEIROS, 1999; NEVES, 2003).

Inside the watershed divides, there are Paleoproterozoic metamorphic rocks from the Belém do São Francisco Complex and Mesoproterozoic rocks from the Cabrobó Unit, which are truncated by Neoproterozoic Granitoids and Plutons at the western edge, with the presence of strike-slip faults. Two batholiths are worth mentioning; Ouro Branco Pluton and Serra do Catu Pluton. After the confluence with the Canapi River, the Capiá carved its valley over the Chocorró intrusive suite and the leucogranites pluton, where the river bends and fits into a steep valley, before emptying at its base level, the São Francisco River bed.

From a geomorphological point of view, the Capiá river watershed is located between the Borborema Plateau and the Sertaneja Depression (Figure 2). The presence of the Borborema plateau in the basin is associated with the headwaters of the Canapi River. However, the outstanding relief that most attracts attention amid the Sertaneja Depression is the Mata Grande Massif. This feature was described by Gois et al. (2021) as a highland humid enclave, that is, a sub-humid area amid a semi-arid environment. With elevations that reach more than 800 meters, this enclave contains the Onça Ridge, one of the high-elevation surfaces of the state of Alagoas. In the watershed, there is the presence of inselbergs that occur isolated or in groups, residual massifs and ridges that stand out through the Sertaneja Depression. In the lower course, near the confluence with the São Francisco river, the Capiá river built a canyon with an altimetric difference of about 100 meters. This feature locally known as "boqueirão", is common to this region (FERNANDES LIMA, 1992).
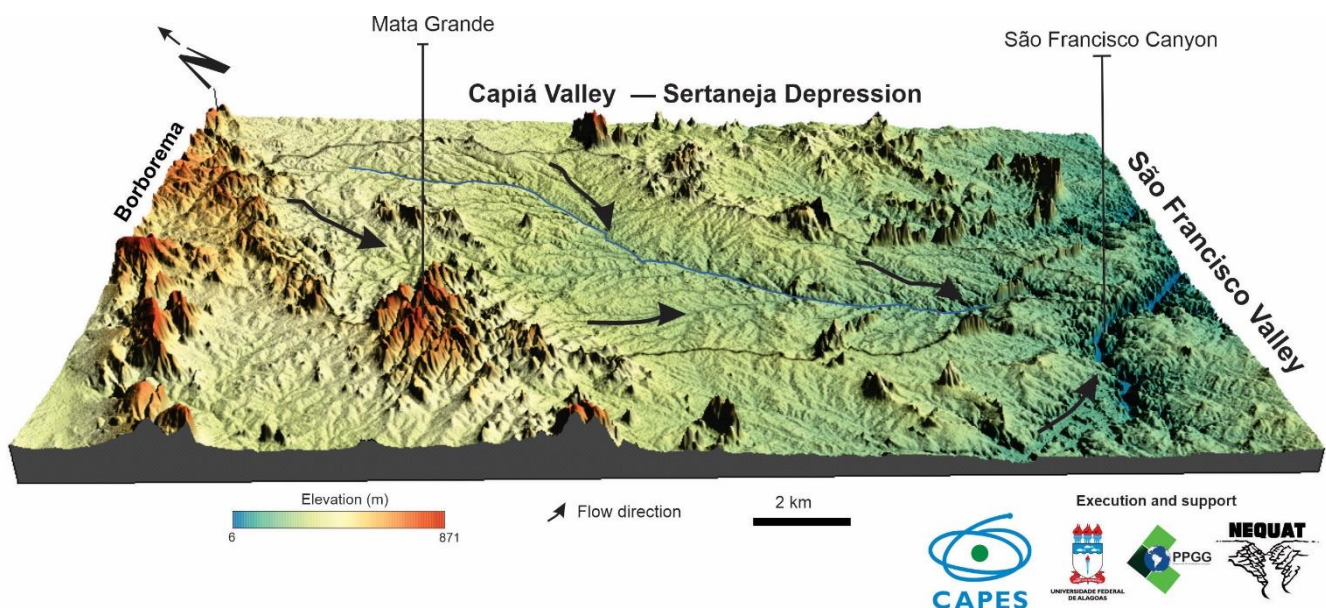

Figure 2. Relief of the Capiá River watershed from Topodata DEM.

3. Materials and Methods

To analyze the eroded topography at the watershed scale over the Proterozoic basement, we used three different morphometric techniques based on the Topodata DEM, made available by the National Institute for Space Research (VALERIANO; ROSETTI, 2012). These are: hypsometric integral and curve, paleosurface and minimum bulk erosion. In addition, topographic swath profiles were used to visualize the data.

3.1 Hypsometric integral and curve

The hypsometric curve is a normalized, proportional and cumulative relationship between the area and elevation of a given watershed (Figure 3). The area contained in the curve became known as the Hypsometric

Integral (HI). This technique was proposed by Langbein (1947) and Strahler (1952) who already suggested the possibility of this approach being useful for the analysis of eroded topography and the degree of development of river valleys. The value of the Hypsometric Integral varies from 0 to 1. While values closer to unity indicate that there are more portions of high elevation terrain, values closer to zero denote a landscape devastated by denudational processes. In basins where the channels have deepened their valleys, leaving proportions of the drainage area with greater relief, they tend to have the highest values that are described by pronounced curves (convex). In addition, information can be extracted from the morphology of the hypsometric curve, where the steepest sectors suggest the presence of regions with greater altimetric amplitudes and steep hillslopes. Therefore, this tool can clarify dominant erosive processes and regional erosion patterns, as well as the equilibrium of channels and hillslopes profiles (*e.g.*, WILLGOOSE; HANCOCK, 1998; MONTGOMERY *et al.* 2001).
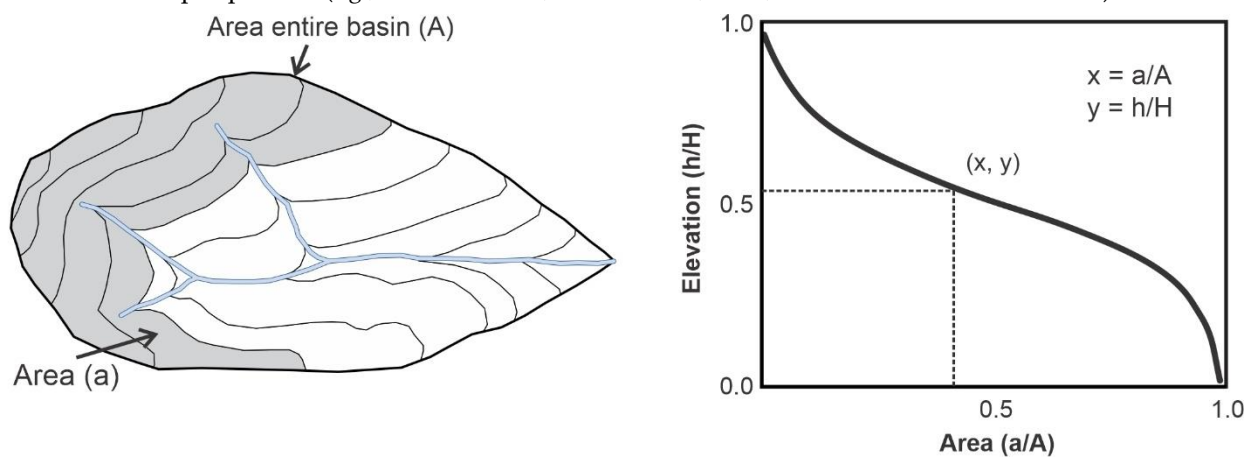

Figure 3. Obtaining the hypsometric integral and curve. Elevation normalization is the ratio of elevation in an altimetric range (h) to the maximum elevation (H) in the catchment area. In the same way, the normalization of the area is made by the quotient between the area contained in an elevation limit (a) and the total area of the drainage basin (A). Adapted from Montgomery and Bierman (2013).

This method, by relating the level of denudation to the hypsometric curve, led to the use of this index as a marker of the evolutionary stage of landscapes. However, as argued by Summerfield (1991), this reasoning is not valid for large basins, where the interaction with tectonic and climatic processes is responsible for expressive changes in the organization of the system. The curve and integral were calculated using Hypsometry Tools (DAVIS, 2019), which reclassifies the DEM into 100 parts, quantifying the surface contained in each elevation interval. The intervals are then normalized concerning the maximum elevation of the basin, while the area contained in each elevation range is normalized concerning the total area of the basin. According to Brocklehurst and Whipple (2004), one can calculate the hypsometric integral (HI) in this way (1):

$$HI = \frac{H_{med} - H_{min}}{H_{max} - H_{min}} \tag{1}$$

Where H_{med}, H_{min} and H_{max} represent, respectively, the average, minimum and maximum elevations of the watershed. To illustrate an ideal erosion cycle, Strahler (1952) proposed that HI values greater than 0.60 are diagnostic of a younger relief, with convex hypsometric curves, values between 0.35 and 0.60 indicate the presence of the maturity or equilibrium stage, whose curves are S-shaped, and, finally, values lower than 0.35 characterize oldest or Monadnock stage, also marked by the maximum concavity of the hypsometric curve (*e.g.*, MONTEIRO; CORREIRA, 2020). However, it should be noted that watersheds from different areas cannot be compared to establish a relationship between the volume eroded through this technique. In this way, the hypsometric integrals represent different absolute denudation levels between drainage basins of different sizes. Therefore, the paleosurface

reconstruction and the minimum bulk erosion were applied.

The drainage basin geometry also influences the HI value. More elongated watersheds tend to have a lower HI value (WILLGOOSE; HANCOCK, 1998). For this reason, the elongation factor (*F*) of the watershed was calculated using the following equation (2), based on Sassolas-Serrayet *et al.* (2018):

$$F = \frac{P_r}{2\sqrt{\pi A_r}} \qquad (2)$$

Where P_r and A_r are, respectively, the perimeter and area of the river basin. This equation compares the perimeter of the basin to a circumference with an equivalent area. Thus, $F = 1$ denotes a perfectly circular basin, while higher values indicate an elongated watershed.

3.2 Minimum Bulk Erosion

Minimum Bulk Erosion (*E_{bulk}*) is the difference between the virtual surface obtained by interpolation of the current elevation of the watershed dividers and the real surface, with the incision of the drainage network (Figure 4). This is an underestimated value, as the divisors were once higher than they are at present. In this case, by convention, the inverse distance weighting method was used as a deterministic interpolator, as guided by Gaidzik and Ramírez-Herrera (2017). With this, it is possible to investigate the pattern and distribution of eroded topography at the watershed scale and compare the results with other parts of the world. Antón, Muñoz-Martín and Vicente (2018) state that the positive values obtained by this subtraction represent surfaces lowered by denudation, while the negative ones are relict topographies.
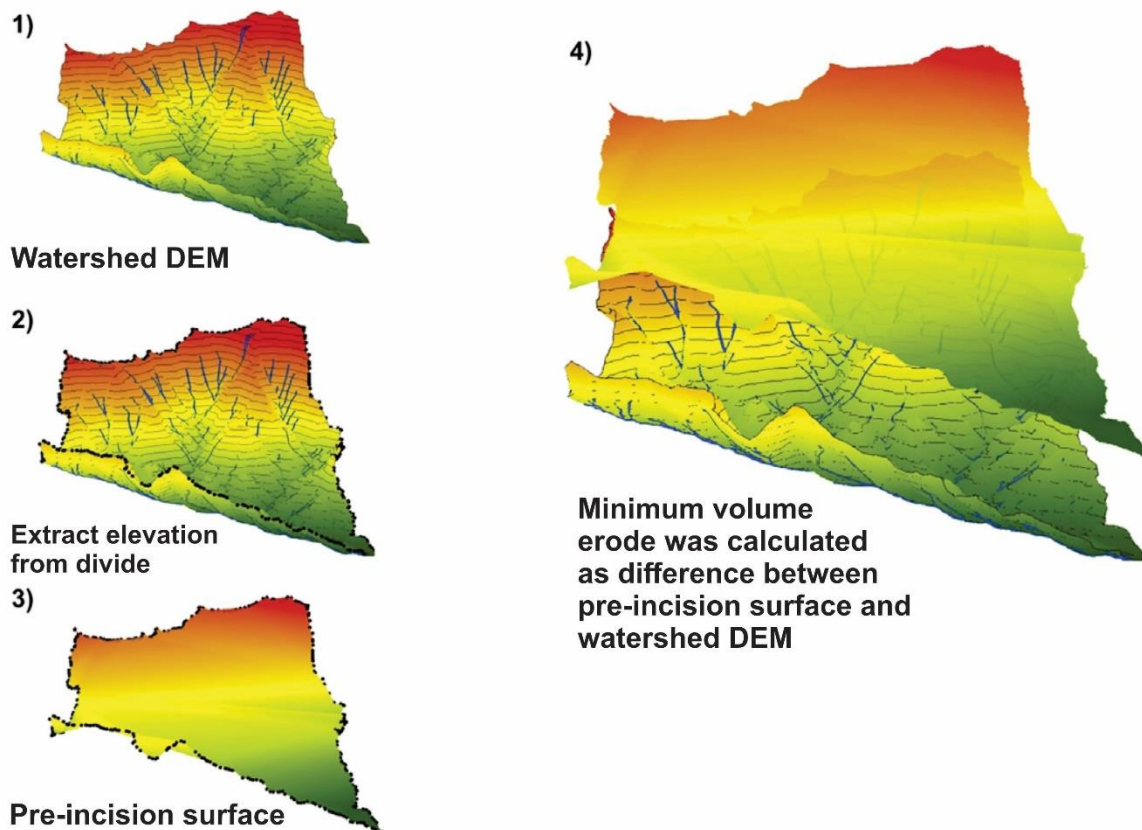

Figure 4. Schematic steps for calculating the E_{bulk}. Adapted from Gaidzik and Ramírez-Herrera (2017).

3.3 Paleosurface

To construct the paleosurface of the Capiá drainage basin, the methodology presented by Tavares (2010) was used, which consists of interpolating spot height from topographic maps or the closure of contour lines generated from the DEM. Following the proposal by Aires *et al.* (2012), to extract the spot height, digital maps at a scale of 1:250,000 from the 1970s, 1980s and 1990s were used, provided by the Army Geographic Database (BDGEx) that were processed in the Geostatistical Wizard software. Ordinary kriging was used because it considers the stationarity of the mean at the local scale and because it has been used to reconstitute topographical meshes in previous studies, showing satisfactory results (*e.g.*, SISKA *et al.* 2005). The semivariance of the data was plotted as a function of the sample distance to construct the semivariogram. Predictive models (*e.g.*, circular, spherical, Gaussian) were compared to then estimate the nugget effect, sill and range (YAMAMOTO; LANDIM, 2013). The model that best fitted the dataset was chosen, considering the optimization of the simple and normalized mean error, in addition to reducing the difference between the input and predicted values. Before applying this technique, the normality of the data was verified using the Shapiro-Wilk test (1965). For the construction of the semivariogram, data normality is desirable, but dispensable (ASSUMPÇÃO; HADLICH, 2017). To compare the difference between the data predicted by the model and those observed in reality, the non-parametric Kruskal-Wallis test was used (KRUSKAL; WALLIS, 1959). These steps were performed in R_studio v.4.0.3 software. The main advantage of using this methodology is the expressive reduction of the drainage incision on the surface, mainly of the drainage headwaters, allowing the delineation of structural blocks with particular characteristics of varied extension.

4. Results and discussion

The morphology of the hypsometric curve demonstrates a mostly concave profile, a morphometric signature of the semiarid pediplans of Northeastern Brazil, elaborated in the Proterozoic basement (Figure 5). From this, the relief was classified as mature, marked by lowered dividers, low-relief and wide river valleys, a stage of equilibrium, as described by Strahler (1952). However, Willgoose and Hancock (1998) asserted that the morphology of this type of curve may be influenced by the geometry of the basin and may not be directly associated with its evolutionary stage, stating that basins with higher elongation factors may exhibit a Monadnock or old stage.

The basin elongation factor was 2.12, considering a perimeter of 364.25 km and a drainage area of 2,344 km². This means that the basin has a high elongation (SASSOLAS-SERRAYET *et al.* 2018) and this factor influences the morphological conformation of the hypsometric curve (*e.g.*, WILLGOOSE; HANCOCK, 1998). This is a topological condition for controlling the shape of the hypsometric curve, but it is not possible to neglect other controls that affect this pattern in the semi-arid plains, especially because it is an area known to have been devastated by denudational processes over tens of millions of years and with structural controls. outstanding (e.g., JELINEK et al. 2014; CORRÊA et al. 2019). Furthermore, it is worth emphasizing the role of lithostructural control in the adjustment of hypsometry. For example, at the scale of the watershed, combining hypsometric data and geology, it is possible to notice that some residual reliefs are constituted by lithologies constituted by the felsic plutonic Serra do Catu unit, such as quartz-syenite (BRITO *et al.*, 2009).

Another important part of the analysis of the eroded topography is the final segment or toe of the hypsometric curve, where there is the convergence of the largest accumulated area and the smallest proportion of elevation. In the case of the Capiá river basin, this segment, which presents an abrupt drop, can be explained by the geometry of the drainage network, based on Willgoose and Hancock (1998). This particularity is then attributed to the subparallel pattern with which the affluents join the trunk stream, as a rule, at different levels. As the Capiá river developed a canyon before joining the São Francisco river, this sign

of disturbance is imprinted on the hypsometric curve. This suggests a recent base level fall and it appears that in this sector the length of the hillslopes has changed as the share of contribution from areas with low elevation has increased (*e.g.*, HUST et al. 2012). This control is related to adjustment mechanisms in response to the base level fall, such as the migration of knickpoints towards the headwaters, as reported by Gallen et al. (2011), in an attempt to couple hillslope processes to the erosive dynamics of bedrock channels in the Appalachians. This process is even more direct in semi-arid regions, where hillslopes are usually described by weathering-limited conditions. In other words, soil removal processes are more efficient than those of deepening the weathering mantle (*e.g.*, PHILLIPS et al. 2019; GOUDIE, 2013).

It can be seen that, like the low-relief surfaces of Central Africa or even drainage basins in the Appalachians (*e.g.*, GUILLOCHEAU *et al*. 2018; GALLEN *et al*. 2011), the frequency distribution by elevation range, illustrated by the histogram in Figure 5, do not show a unimodal distribution for the Capiá river basin. There are, at least, three frequency peaks. The first peak has an elevation corresponding to ≤ 223 m, the second is ≤ 270 m and the third is ≤ 382 m. These intervals of higher cumulative relative frequency correspond to 22%, 33% and 47%, respectively, of the total area of the watershed. Although the first frequency peak appears in the sequence of the elevation bands in which the Capiá River canyon is covered, the other two cannot be explained based on the presence of this feature. While there are signs of transition in this landscape, such as the presence of knickpoints in the longitudinal profiles of the river network (FERNANDES LIMA, 1992; NASCIMENTO, 2020), the other frequency peaks may be related to the leveling of erosion surfaces or the maintenance of surfaces by lithological contrast. However, no large scarps are delimiting the pediment levels, which does not exclude the possibility that these surfaces were established at different ages and conditions. Another possible interpretative alternative is the reactivation of basement structures, which are also correlated with elevated terrains in the upper course of the Capiá River basin, with a notable emphasis on the Itaíba fault, which roughly delimits the restricted presence of the Borborema Plateau in the basin, at the north of the city of Canapi, on the upper course of the Capiá river.
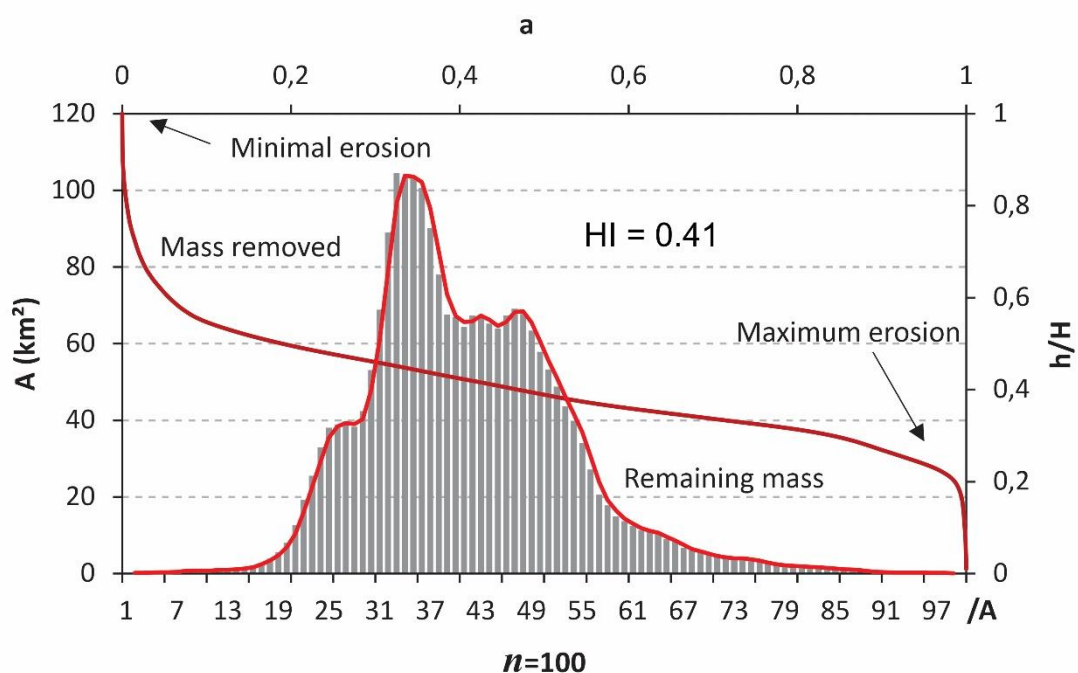

Figure 5. Curve, hypsometric integral and frequency distribution of the elevation ranges (*n* = 100) for the Capiá river basin. The red outlining the frequency histogram is the moving average considering two-element steps. Note that the frequency distribution is multimodal.

The hypsometric integral of the watershed was calculated and 0.41 was obtained (Figure 5) which corresponds to the equilibrium or maturity stage described by Strahler (1952). If the paleotopography of the watershed were characterized by a solid block (1:1), with a hypsometric integral value close to unity, about 59% of the mass of the initial topography would have been eroded. The remaining topography may have been maintained by differential erosion (*e.g.*, SACEK *et al*., 2019) or may be taken as an indication of rejuvenation (GURGEL *et al.* 2013). Despite the drainage basin landscape being predominantly marked by a pediplan, according to the assumptions of Schumm (1956) and Strahler (1952), these surfaces would be characteristic only of the low fluvial course, with a proportion of mass removed close to unity. However, Willgoose and Hancock (1998) warn of the sensitivity of the scale factor within this analysis. Watersheds of primary orders tend to have a hypsometric integral close to the unit and this indicates the predominance of hillslope processes to the detriment of fluvial erosion. Montgomery *et al*. (2001) reaffirm this principle, noting that hypsometry varies consistently with the prevailing erosion processes. In the study area, the river erosion process is mainly controlled by bedload abrasion (*e.g.*, CHATANANTAVET; PARKER, 2009). Similar to what occurs in the longitudinal profiles of bedrock rivers, it is expected that, over geological time, the region of maximum erosion will migrate towards the headwaters, reducing the mass available for denudation and the hypsometric integral of the Capiá river basin.
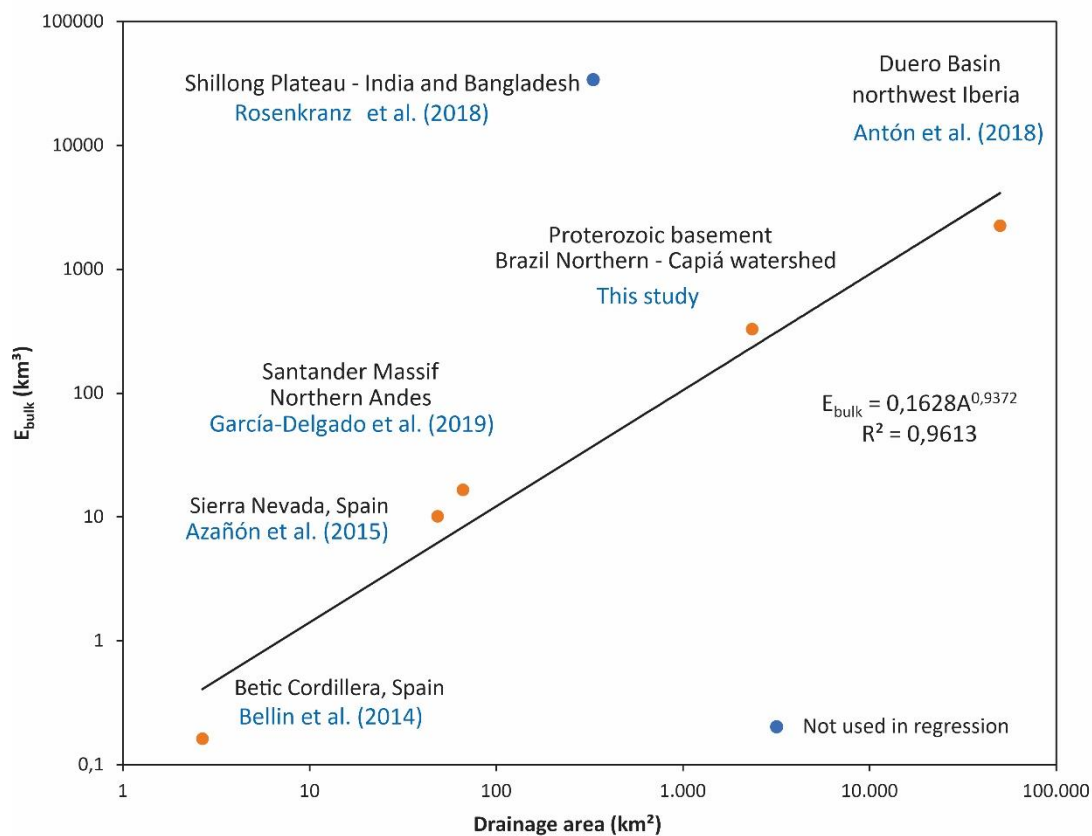

Figure 6. Bilogarithmic comparison between minimum bulk erosion and mean drainage area in previously published studies. It is noted that there is a dependence on the drainage area, but as the controls in the geomorphological system are multivariate, not all regions follow this trend, as illustrated by the Shillong Plateau, between India and Bangladesh.

Although allowing the comparison of different watersheds, as it is a normalized index, the curve and hypsometric integral do not provide the real or absolute dimensions of the eroded volume. Thus, to overcome this

limitation, the calculation of the Minimum Bulk Erosion (E_{bulk}) was also used. It is reiterated that this estimate is a minimum value, as the methodology considers the current elevation of the divide as a starting point, but these have also been lowered over geological time, though at a different rate than the river valleys (BROCKLEHURST; WHIPPLE, 2002; SMALL; ANDERSON, 1998; GILBERT, 1909). The E_{bulk} calculated for the Capiá River basin was 329 km³ or 1.4×10^5 m³/km². Although substantial, this value is still modest compared, for example, to those calculated by Atón, Muñoz-Martín and Vicente (2018) in the Douro River basin, in the Iberian Peninsula. The authors calculated 2251 ± 524 km³ of eroded volume in an area of approximately 50 thousand km² (about 25 times larger than the Capiá river basin), estimated from the elevation of neogenous deposits. Meanwhile, Rosenkranz *et al*. (2018) estimated 7.9×10^{10} m³/km² of E_{bulk} in the Shillong Plateau, between India and Bangladesh, which is considered the wettest place on the planet (7 to 12 m/year). This contrast between the volume eroded in semi-arid and extremely humid regions can be taken as an example of the imbricated relationship between climate and terrestrial modeling. One can also note the contrast with the data from Sierra Nevada, Spain, with 16×10^7 m³/km² of E_{bulk} and documented fault and fold control (AZAÑÓN *et al*. 2015). Another important point is that comparing the data already published with those presented in this study (Figure 6), it can be seen that there is a positive tendency for the E_{bulk} to increase with the drainage area, even in contrasting areas of the globe. It is noteworthy that, although the relationship between drainage area and eroded volume in the study region has a comparatively high absolute E_{bulk}, in terms of erosion volume per area, this value is lower compared to other regions of the world, especially in active tectonic setting and with higher average annual precipitation rates.
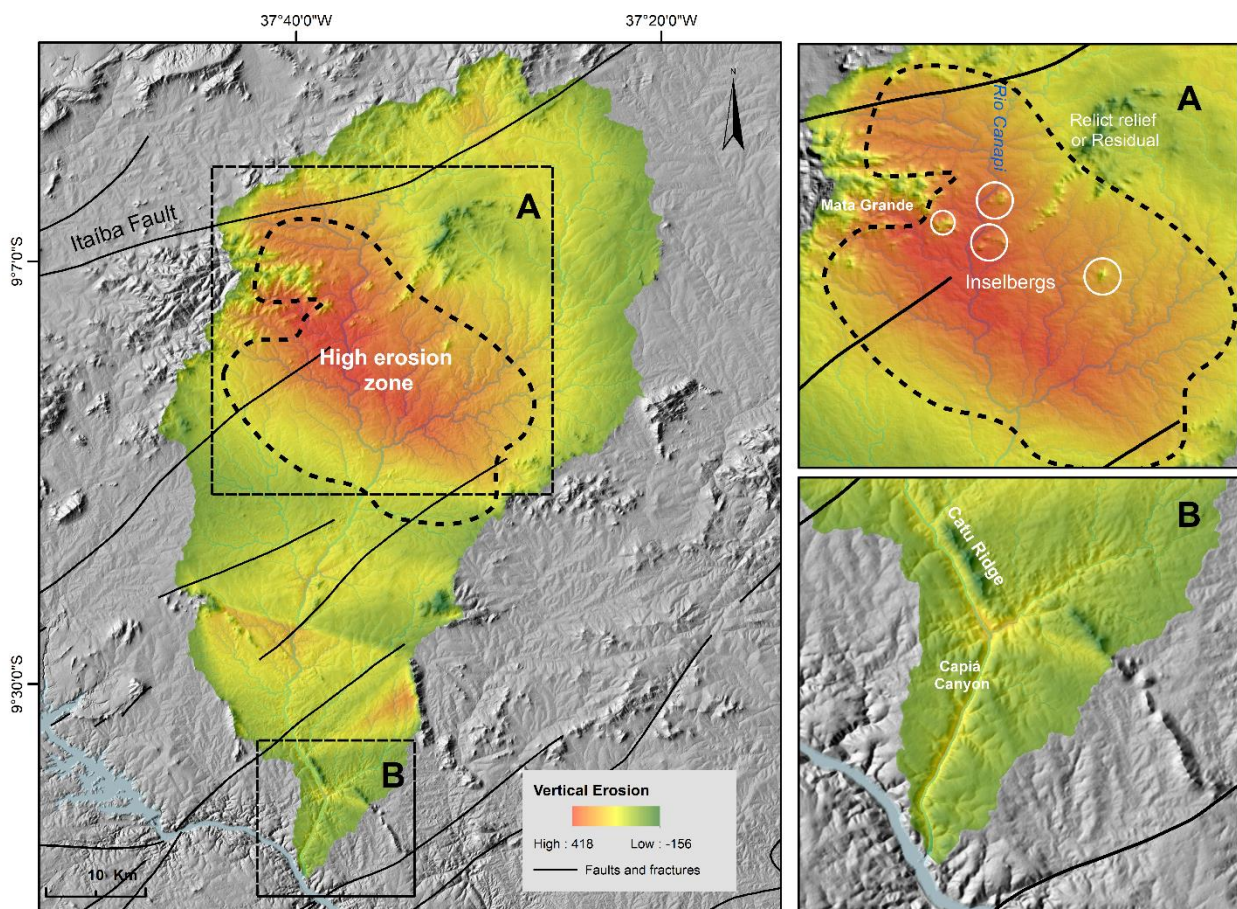

Figure 7. Spatialization of the vertical incision in the Capiá River Basin. Note the presence of relict and residual landforms (A), such as ridges (Catu ridge) and *inselbergs*, in addition to the Capiá canyon (B) before the confluence with the São Francisco River.

With the reconstituted pre-incision surface subtraction from the elevation of the water dividers, the spatialization of columnar or vertical erosion was also obtained for each raster cell delimited by the area of the Capiá river basin, with a maximum of 418 and a minimum of -156 (Figure 7). Values less than zero are associated with denudated relict topographies that currently find elevations above the first-order dividers, suggesting that the rates of denudational processes over them are lower than in the surrounding landscape. These areas are normally structured by rocks with a higher degree of resistance, evidencing the role of differential erosion in their persistence. In the study area, these features represent residual ridges and massifs that, according to Twidale and Borne (2013a, b), have their origin linked to the deepening and removal of weathering mantles, especially in granitic terrains, as in the study area presented here. With the greatest amplitude between the bottom of the valleys and the dividers, a wide pocket of vertical erosion has developed between the Capiá and Canapi rivers, where an abundance of inselbergs can be found. It is in the vicinity of this feature that the Onça ridge is located, one of the high-elevation surfaces of the lower course of the São Francisco River. According to Gois *et al.* (2021), this area is in a different context from the entire surroundings, with environmental characteristics that allow it to be classified as a highland humid enclave amid semi-arid pediments (Figure 8).
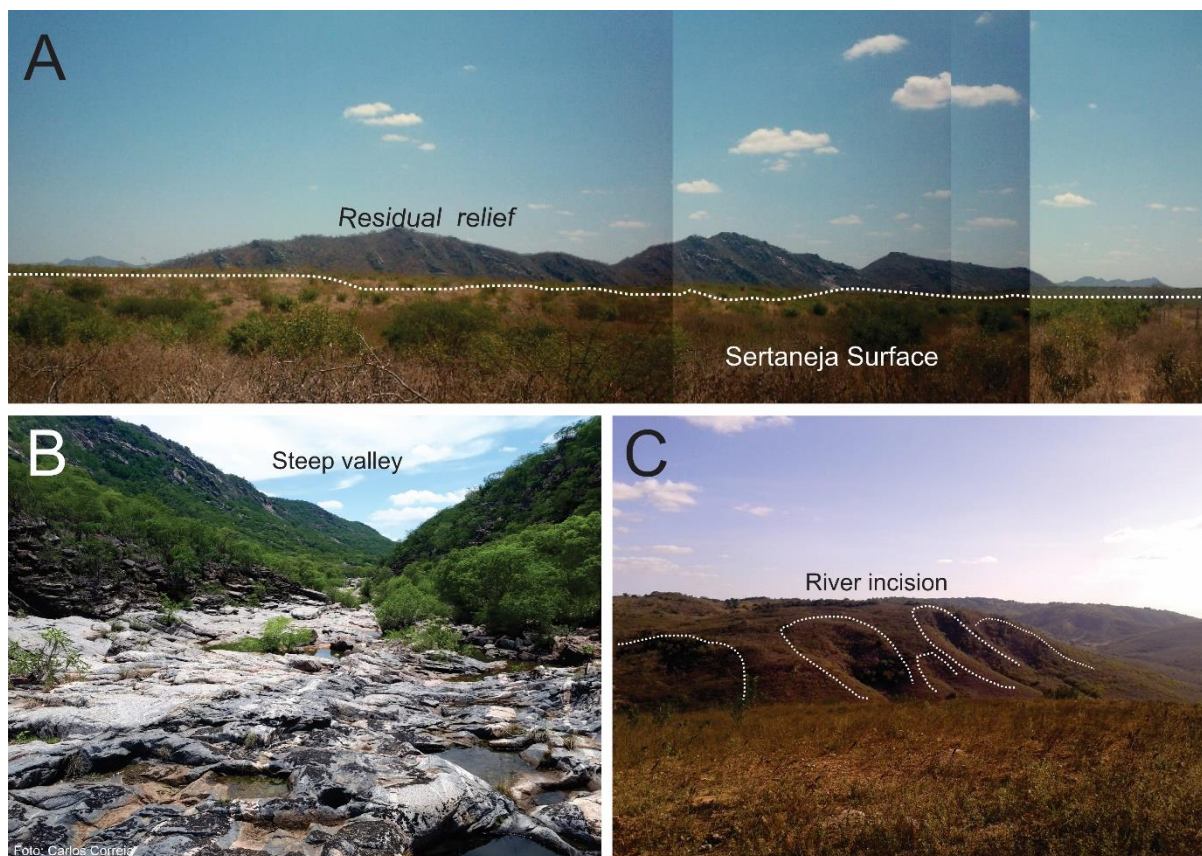

Figure 8. Expression of structural controls in the study area. Residual ridge (Catu Ridge) emerges amidst the pediments that form the Sertaneja Surface (A). Capiá river canyon with an altitude difference of about 100 meters (B). Linear erosion features on the hillslopes of the Mata Grande highland (C).

Giaconia et al. (2012) found up to 389 meters of vertical erosion in basins draining the Sierra Alhamilla, Spain, while Small and Anderson (1998) in the Laramide Mountains in the United States estimated up to 1 km of vertical erosion, averaging 300 m, about. In comparison, the average vertical incision in the Capiá river basin is 140 m, less than half the value found by Small and Anderson (1998) in another geodynamic context. As verified for the

eroded volume, there is also a dependence on the drainage area about the vertical incision, as presented by Brocklehurst and Whipple (2002). This is a direct consequence of the predominance of river activity in non-glacial erosive landscapes (HOWARD et al., 1994). It is also worth noting that the surface with greater vertical erosion is limited by faults on its flanks, such as the Itaíba Fault and the transcurrent faults system in the middle course of the Capiá River. This may even be evidence that these structures and their branches act as plans of weakness for the long-term erosion of the crystalline shield, as documented by Maia and Bezerra (2020) for the Northern Northeast. In this sense, the morphometric parameters suggest that this sector is affected by controls different from those that operate throughout the rest of the river basin.

For paleosurface reconstruction, elevation data from 1069 spot heights were processed on topographical maps at a scale of 1:250,000. The data present an amplitude of 801 m, with a minimum elevation of 41 m and a maximum of 844 m. The mean elevation was 370 ± 158 m (σ). To avoid undesirable edge effects, it was decided to select points for a rectangle that would cover the area of the Capiá River basin and its surroundings. The kurtosis, which is a measure of flattening between the data distribution and the normal curve, was -0.38. This value allows classifying it as platykurtic, that is, the data distribution curve is smaller than the normal distribution (ANDRIOTTI, 2003). The asymmetry coefficient was 0.36, which can be interpreted as a positive asymmetry and the maximum frequency of the values is concentrated relatively closer to the origin, with a smooth "tail" to the right (LARSON, 2010). After calculating the descriptive statistics of the data set, the Shapiro-Wilk (1965) normality test was applied, in which the null hypothesis is that the data follow the standard normal distribution. At a significance level of 5%, it was found that the data do not follow a normal distribution ($p < 0.05$). Even so, ordinary kriging was applied, because according to Assumpção and Hadlich (2017), this condition is not necessary for the construction of the semivariogram. It is more important for the construction of the model that the data are reasonably symmetrical, admitting the necessary assumptions, such as the stationarity of the mean.
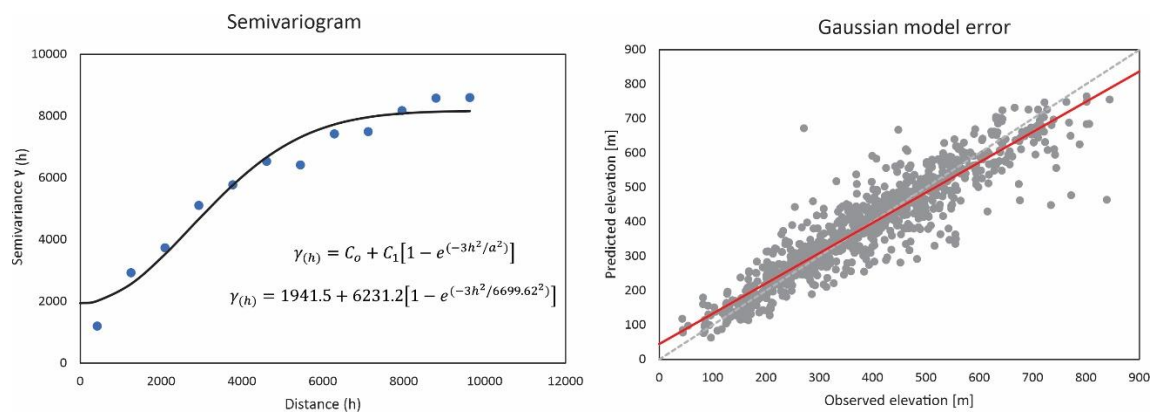

Figure 9. Semivariogram fitted to the data and error of the Gaussian model (red line) compared to the theoretical 1:1 fit line (dashed line). In the model C_o represents the nugget effect, C_1 symbolizes the sill, h is the distance (in meters) and a is the range.

Through the optimization of the semivariogram parameters (Figure 9), it was concluded that the best fit of the data was produced by the application of the Gaussian model, with the morphology of the curve in sigmoid, which resulted in a difference between the mean standard error and mean error quadratic of 0.80. This statistic is obtained through cross-validation, which consists of excluding each measured point — one at a time — from the set, while its measurement is estimated by the model based on the remaining points (ISAAKS; SRIVASTAVA, 1989). As can be seen in Figure 8, the semivariance ($\gamma_{(h)}$) shows an evident dependence on the inter-sample distance (h). It can also be observed that the theoretical model fits omnidirectional real data, with 0° angular direction and 90° tolerance (*e.g.*, ASSUMPÇÃO; HADLICH, 2017), with a tendency to overestimate values smaller than 400 m and overestimate values from this point on the threshold (Figure 8). The Kruskal-Wallis test allowed us to conclude that the difference between predicted and observed data is statistically insignificant at a significance level of 5% ($p > 0.05$). The average prediction error was 0.52

and ideally this value should be closer to zero. The range of the model was 6700 m. The sill was 6231 and the nugget effect was 1942 (C_1). This high nugget effect value (C_0) can be attributed to the sampling scale and the spatial variation of the elevation. The degree of randomness of the data, defined by Yamamoto and Landim (2013) as the quotient between C_0 and C_1, was 0.31, being classified as very random.

The input data, used for the construction of the pre-river incision or paleosurface, managed to eliminate mainly the topographic influence of the first and second-order channels. In the upper part of the basin, the highest elevations are located, especially over Mata Grande and in the Borborema plateau extension in the watershed. Predictably, in locations that have a higher density of sampled points, there is also a lower standard error (Figure 10). According to Siska et al. (2005), the errors associated with ordinary kriging are also correlated with terrain properties in a given region and concluded that the increase in roughness significantly affects the obtained estimates. The paleosurface also allowed the sectioning of two large geomorphological compartments at the basin scale. The highest surface is associated with the upper course of the Capiá river and its Canapi tributary, being roughly delimited by lines of crustal discontinuity, above 500 m, with an oblique NE-SW direction. The other surface is that of the Sertaneja Depression, which is the most pervasive and devastated by denudational processes and the omnipresence of residual reliefs, which cut Proterozoic rocks. A swath profile was constructed to highlight the difference between the current and reconstructed topography and lithostructural controls (Figure 10).
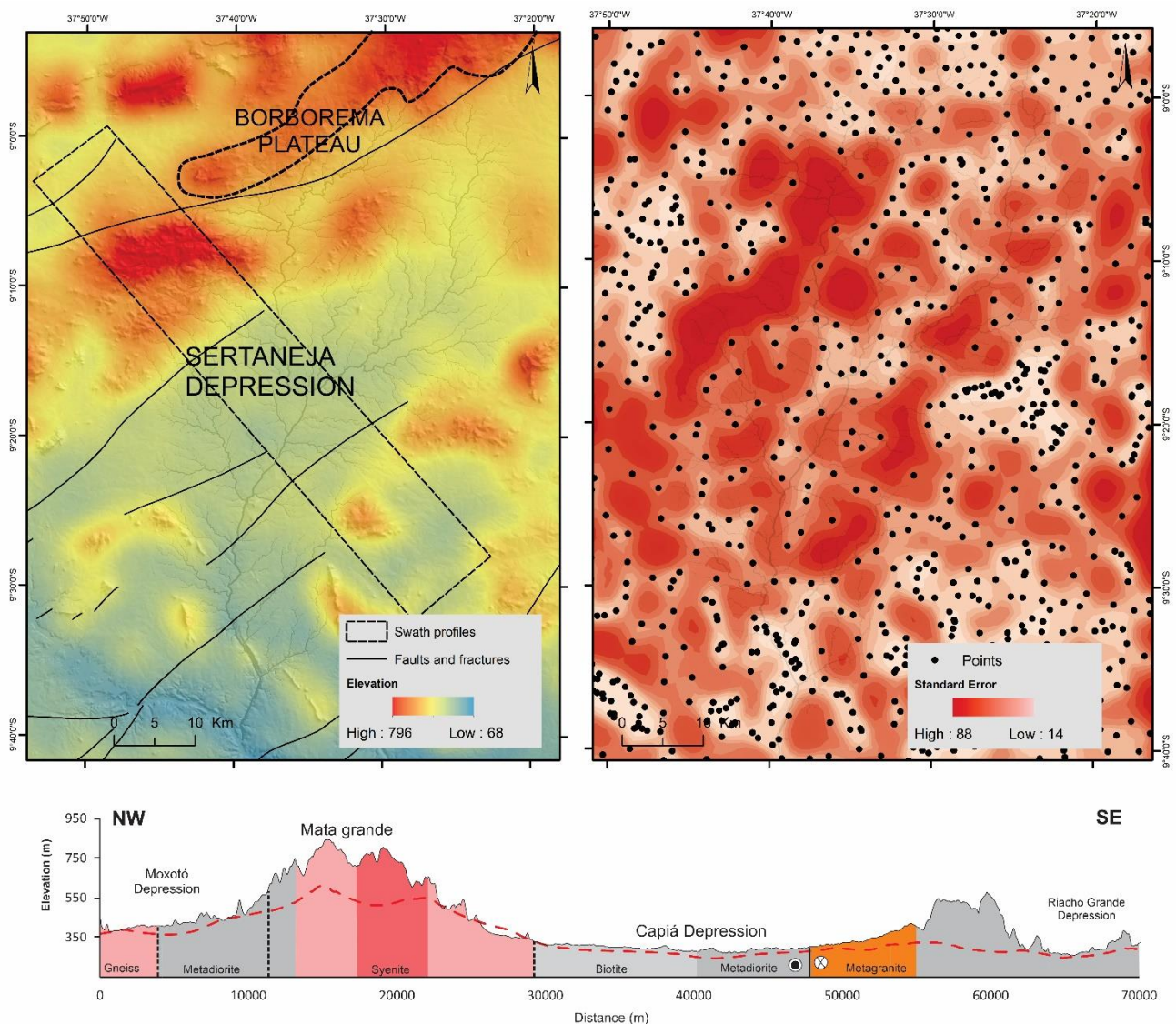

Figure 10. The map above represents the paleosurface or pre-incision surface, on the left, obtained by ordinary kriging. On the right, standard error of the interpolation process, where in places without measurement there is greater uncertainty of the predicted value. Then, the swath profile with the maximum elevations currently found compared to the minimum elevations obtained by the paleosurface reconstruction (dashed red line). The underlying geology was adapted from Medeiros (2000).

The swath profile was 12 km wide and 70 km long. The maximum elevation of the modern topography and the minimum reconstructed were plotted, where the geology of the substrate was also illustrated. The largest amplitudes (> 200 m) are found at the dividers of the Capiá, Moxotó and Riacho Grande river basins (Figure 10). On the western flank, the highest relief amplitudes are found in the Mata Grande Massif, structured on Neoproterozoic syenites. On the eastern side, metadiorites structure an outstanding residual relief. It cannot be ignored, therefore, that, especially in Mata Grande, there are indications that the combination of lithological resistance to denudational processes and possible deformations, associated with the presence of faults in their adjacencies, may be responsible for the persistence of the relief with similar elevation to the Borborema Plateau, to the north. However, there are still no studies of the kinematics of the faults that surround this massif, much less evidence of recent activity. According to Tavares (2010) and Monteiro (2010), for the topographical thresholds established by King (1957), in the study domain, there are intermediate levels of planation, with elevations between 650 and 950 meters, called South American surface or Borborema by Mabesoone and Castro (1975) and lower levels, with elevations between 650 and 100 meters corresponding to the Velhas or Sertaneja surface. Below these levels, there is the current erosion cycle, representing the establishment of river valleys, called the Paraguaçu Cycle. The topo-chronological relationships proposed based on the identification of these flattened surfaces are not valid for the entire extension of the northeastern landscapes, as already argued by Maia, Bezerra and Claudino-Sales (2008) and Maia, Bezerra and Claudino-Sales (2010).

Planation surfaces are one of the basic paradigms that give rise to deep debates within Geomorphology, especially in the Northeast of Brazil (MONTEIRO, 2010). For Ab'saber (1956), the peripheral and semi-arid depressions of the Northeast that surround the Borborema Plateau would have been formed by intense denudational processes of Mesozoic (Triassic and Cretaceous) covers, concomitant with the epirogenesis responsible for forming the Borborema Plateau and the establishment Atlantic as a general base level. The author writes that "from Palmeiras dos Índios", east of the Capiá river basin, "up to the slopes of the Tacaratú plateaus, it extends (...) depressed and low-lying areas, corresponding to the peripheral depression elaborated in the southern portion of the Borborema" (p.4). With advances in geochronological techniques, recent works have reformulated the understanding of the evolution of the northeastern relief and the Brazilian continental margin.

There are studies of apatite fission trace in the study domain, such as those by Japsen *et al*. (2012), Jalinek (2014) and Turner *et al*. (2008), who interpret the data differently. Corrêa *et al*. (2016) warn that these data do not have adequate resolution to detect recent crustal movements and that they are used with greater reliability to elucidate denudational events with more than 1 Ma, highlighting their importance for estimating erosion rates. Considering the temporal break that separates the age of the rocks and the morphology they exhibit, it is still a challenge to date erosive landscapes. Turner et al. (2008) identified two main episodes of cooling in the region. The first event dates from the Albian (110-100 Ma) and is correlated to the denudation linked to the rifting process between the South American and African continental margins and the second to the process of crustal shortening and post-rift sedimentation of the Bartonian-Tortonian (40-10 Ma).

Japsen *et al.* (2012) reiterate the role that the rifting of the Atlantic margin had on the denudation of intraplate terrains and enumerate four events of episodic cooling that begin at 120 Ma, entering the Campanian, Eocene and Miocene. However, there is still a lot of uncertainty in the shorter cooling intervals. Jelinek et al (2014) and Jelinek (2019) did not find cooling during the Eocene described by Japsen *et al*. (2012). Thus, given the erosive scenario of the northeastern landscapes, with Cretaceous and Cenozoic denudation rates that vary spatially and vertically between 300 and 2000 meters, there are few prospects of identifying regional planation surfaces (JELINEK *et al*. 2014; JELINEK, 2019). It is also assumed that a more parsimonious model than those already proposed for the geomorphological evolution of the Northeast is presented. Jelinek et al (2014) and Jelinek (2019) expose a series of weaknesses in the model that assumes regional planation surfaces and claim that apatite fission trace data do not support this assumption. On the contrary, the data demonstrate that, even at similar levels, several blocks followed particular evolutionary paths of exhumation and erosion. In this perspective, the current forms are the result of complex erosive processes that have had a wide spatial variation and the attempts to find a single answer to the evolution of continental relief be unsustainable.

5. Conclusions

The quantification and spatialization of the fluvial incision through the integration of geoprocessing techniques, geostatistics and orbital remote sensing products proved to be satisfactory and brought new information to the Southern Sertaneja Depression, especially in the lower course of the São Francisco River. As

data on modern erosion rates in the presented landscape are not yet available, this research avenue becomes even more attractive. The hypsometric integral quantification curve showed that approximately 60% of the initial mass of the basin was removed by denudational processes, while it records an episode of recent base level fall in the lower part of the drainage basin, in contact with the São Francisco River.

The reconstitution of the paleosurface using ordinary kriging was satisfactory and eliminated the topographic signal of the first and second-order channels, allowing the accurate delimitation of two large morphostructural compartments in the basin: the Borborema Plateau and Sertaneja Depression. The minimum bulk erosion was presented as an important technique for comparing erosion as a function of the drainage area, placing the investigation in a broader context through data available in the literature. In absolute terms, it was found that one of the largest volumes ever published was recorded, but normalizing the values by area, it was noted that this relationship is surprisingly lower than the data from mountainous regions, by several orders of magnitude. The swath profile, associated with geological information, allowed us to correlate the reconstituted surface and compare it with the current topography, also suggesting structural controls.

Finally, it reiterates the need to carry out geochronological studies that seek to quantify modern rates of erosion in the region, given the difficulty in finding a relationship between the information obtained by apatite fission trace and the modern relief, also taking into account the peculiarities of the semi-arid climate and its associated morphology, such as pediments in the Proterozoic basement.

References

1. AB'SABER, A. N. Participação das superfícies aplainadas nas paisagens do nordeste brasileiro. **Geomorfologia**, n. 19, 1969.

2. AIRES, J. R. *et al*. Análises Geomorfológicas do Platô de Teresópolis e da Serra do Mar, RJ, com o Auxílio de Seppômen e ASTER GDEM e sua Relação aos Tectonismos Cenozoicos. **Anuário do Instituto de Geociências**, v. 35, n. 2, 2012.

3. ANDRADES FILHO, C. O.; ROSSETTI, D. F. Caracterização morfoestrutural da parte central emersa da bacia Paraíba (PB). **Geociências** (São Paulo), v. 31, n. 1, 2012.

4. ANDRIOTTI, J. L. S. **Fundamentos de Estatística e Geoestatística**. São Leopoldo: Editora Unisinos, 2003.

5. ANTÓN, L.; MUÑOZ-MARTÍN, A.; VICENTE, G. Quantifying the erosional impact of a continental-scale drainage capture in the Duero Basin, northwest Iberia. **Quaternary Research**, v. 91, n. 2, 2019.

6. ASSUMPÇÃO, H. C. P.; HADLICH, G. M. Estatística descritiva e estacionaridade em variáveis geoquímicas ambientais. **Engenharia Sanitaria e Ambiental**, v. 22, n. 4, 2017.

7. AZAÑÓN, J. M. *et al*. Relief and drainage evolution during the exhumation of the Sierra Nevada (SE Spain): Is denudation keeping pace with uplift?. **Tectonophysics**, v. 663, p. 19-32, 2015.

8. BELLIN, N. *et al*. Denudation rates and tectonic geomorphology of the Spanish Betic Cordillera. **Earth and Planetary Science Letters**, v. 390, 2014.

9. BONNET, S. *et al*. Large-scale relief development related to Quaternary tectonic uplift of a Proterozoic-Paleozoic basement: The Armorican Massif, NW France. **Journal of Geophysical Research**: Solid Earth, v. 105, n. B8, 2000.

10. BRITO, M. F. L.; SILVA FILHO, A. F.; PINHO GUIMARÃES, I. Caracterização geoquímica e isotópica do batólito Serra do Catu e sua evolução da interface dos domínios Sergipano e Pernambuco Alagoas, Província Borborema. **Brazilian Journal of Geology**, v. 39, n. 2, 2009.

11. BROCKLEHURST, S. H.; WHIPPLE, K. X. Glacial erosion and relief production in the Eastern Sierra Nevada, California. **Geomorphology**, v. 42, n. 1-2, 2002.

12. BROCKLEHURST, S. H.; WHIPPLE, K. X. Hypsometry of glaciated landscapes. **Earth Surface Processes and Landforms**, v. 29, n. 7, 2004.
13. CHATANANTAVET, P.; PARKER, G. Physically based modeling of bedrock incision by abrasion, plucking, and macroabrasion. **Journal of Geophysical Research**: Earth Surface, v. 114, n. F4, 2009.
14. CORRÊA, A. C. B. *et al*. The Semi-arid Domain of the Northeast of Brazil. In: SALGADO, A. A. R. *et al*. (orgs). **The Physical Geography of Brazil**. Spring, 2019.
15. CORRÊA, A. C. B.; MONTEIRO, K. A. Revisitando as superfícies de aplainamento: novos enfoques e implicações para a geomorfologia geográfica. **Humboldt**, v. 1, n. 2, 2021.
16. DAVIS, J. **Hypsometry Toolbox**. Disponível em: <https://gis.sfsu.edu/content/hypsometry-tools>. Acessado em 01 de dezembro, 2019.
17. GAIDZIK, K.; RAMÍREZ-HERRERA, M. T. Geomorphic indices and relative tectonic uplift in the Guerrero sector of the Mexican forearc. **Geoscience Frontiers**, v. 8, n. 4, 2017.
18. GALLEN, S. F. *et al*. Hillslope response to knickpoint migration in the Southern Appalachians: implications for the evolution of post-orogenic landscapes. **Earth Surface Processes and Landforms**, v. 36, n. 9, 2011.
19. GIACONIA, F. *et al*. Geomorphic evidence of active tectonics in the Sierra Alhamilla (eastern Betics, SE Spain). **Geomorphology**, v. 145, p. 90-106, 2012.
20. GILBERT, G. K. **Report on the Geology of the Henry Mountains**. US Government Printing Office, 1877.
21. GILBERT, G. K. The convexity of hilltops. **The Journal of Geology**, v. 17, n. 4, 1909.
22. GODARD, A. *et al.* (eds). **Basement regions**. New York: Springer, 2001.
23. GOIS, L. S. S. *et al*. Caracterização sedimentológica dos colúvios do maciço de Mata Grande–AL: uma comparação entre brejos de altitude do Nordeste do Brasil. **Revista de Geociências do Nordeste**, v. 7, n. 1, 2021.
24. GOUDIE, A. S. **Arid and semi-arid geomorphology**. New York: Cambridge University Press, 2013.
25. GRAF, W. L. **Fluvial processes in dryland rivers**. New York: Springer-Verlag, 1988.
26. GUILLOCHEAU, F. *et al*. Planation surfaces as a record of mantle dynamics: the case example of Africa. **Gondwana Research**, v. 53, 2018.
27. GURGEL, S. P. P. *et al*. Cenozoic uplift and erosion of structural landforms in NE Brazil. **Geomorphology**, v. 186, 2013.
28. HASUI, Y. *et al*. (Ed.). **Geologia do Brasil**. São Paulo: Beca, 2012.
29. HOWARD, A. D. A detachment-limited model of drainage basin evolution. **Water resources research**, v. 30, n. 7, 1994.
30. HURST, M. D. et al. Using hilltop curvature to derive the spatial distribution of erosion rates. **Journal of Geophysical Research**: Earth Surface, v. 117, n. F2, 2012.
31. ISAAKS, E. H.; SRIVASTAVA, M. R. **Applied geostatistics**. New York: Oxford University Press, 1989.
32. JAPSEN, P. *et al*. Episodic burial and exhumation in NE Brazil after opening of the South Atlantic. **GSA Bulletin**, v. 124, n. 5-6, p. 800-816, 2012.
33. JELINEK, A. R. *et al*. Denudation history and landscape evolution of the northern East-Brazilian continental margin from apatite fission-track thermochronology. **Journal of South American Earth Sciences**, v. 54, 2014.
34. JELINEK, A. R. Evolução paleotopográfica da margem continental brasileira durante o Fanerozoico: evidências a partir da termocronologia por traços de fissão em apatitas. **Revista Brasileira de Geografia Física**. Recife. Vol. 12, n. 4 (2019), p. 1670-1686, 2019.
35. KING, L. C. A geomorfologia do Brasil Oriental. **Revista Brasileira de Geografia**, v.18, n.2, 1957.
36. KRUSKAL, W. H.; WALLIS, W. A. Use of ranks in one-criterion variance analysis. **Journal of the American Statistical Association**, v. 47, n. 260, p. 583-621, 1952.
37. LANGBEIN, W. B. *et al*. Topographic characteristics of drainage basins. **U. S. Geol. Survey**, 1947.
38. LARSON, R. **Estatística Aplicada**. São Paulo: Pearson Prentice Hall, 2010.
39. LIMA, I. F. **Estudos geográficos do semiárido alagoano**: bacias dos rios Ipanema, Traipu, Capiá e adjacentes. Maceió: Governo do Estado de Alagoas, 1992.
40. MABESOONE, J. M. **Sedimentary basins of northeast Brazil**. Departamento de Geologia, Centro de Tecnologia. Universidade Federal de Pernambuco, 1994.
41. MABESOONE, J. M.; CASTRO, C. Desenvolvimento Geomorfológico do nordeste brasileiro. **B. Soc. Geol. Núcleo Nordeste**, v.3, p.5-36, 1975.
42. MAIA, R. P.; BEZERRA, F. H. R.; SALES, V. C. Geomorfologia do Nordeste: concepções clássicas e atuais acerca das superfícies de aplainamento nordestinas. **Revista de Geografia** (Recife), v. 27, n. 1. Esp, p. 6-19, 2010.
43. MAIA, R. P.; BEZERRA, F. H.; CLAUDINO-SALES, V. C. Vales Fluviais do NE: Considerações Geomorfológicas. **Okara**: Geografia em Debate (UFPB), 2008.
44. MAIA, R.; BEZERRA, F. **Structural Geomorphology in Northeastern Brazil**. Springer International Publishing, 2020.

45. MONTEIRO, K. A. **Superfícies de aplainamento e morfogênese da bacia do rio Tracunhaem, Pernambuco**. Dissertação de Mestrado em Geografia. Recife: UFPE, 2010.

46. MONTEIRO, K. A.; CORRÊA, A. C. B. Application of morphometric techniques for the delimitation of Borborema Highlands, northeast of Brazil, eastern escarpment from drainage knick-points. **Journal of South American Earth Sciences**, v. 103, p. 102729, 2020.

47. MONTGOMERY, D. R.; BALCO, G.; WILLETT, S. D. Climate, tectonics, and the morphology of the Andes. **Geology**, v. 29, n. 7, p. 579-582, 2001.

48. MONTGOMERY, D. R.; BIERMAN, D. R. **Key concepts in Geomorphology**. Nova Iorque: W. H. Freeman and Company Publishers, 2013.

49. NASCIMENTO, J. P. H. **Aplicação de índices morfométricos para identificação de controles estruturais atuantes em bacias hidrográficas do Baixo São Francisco**. Dissertação de Mestrado em Geografia. Maceió: UFAL, 2020.

50. NEVES, S. P. Proterozoic history of the Borborema province (NE Brazil): Correlations with neighboring cratons and Pan-African belts and implications for the evolution of western Gondwana. **Tectonics**, v. 22, n. 4, 2003.

51. OLIVEIRA, G. P. *et al*. Compartimentação geomorfológica do maciço de Martins-Portalegre-NE do Brasil. **Revista Contexto Geográfico**, v. 3, n. 6, 2018.

52. ORME, A. R. Denudation, planation, and cyclicity: myths, models, and reality. In: **Treatise in Geomorphology**, v. 1, p. 11-36, 2013.

53. PEULVAST, J. P.; SALES, V. C. Aplainamento e geodinâmica: revisitando um problema clássico em geomorfologia. **Mercator**, v. 1, n. 1, 2002.

54. PHILLIPS, J. D.; PAWLIK, Ł.; ŠAMONIL, P. Weathering fronts. **Earth-Science Reviews**, v. 198, 2019.

55. ROSENKRANZ, R. *et al*. Coupling erosion and topographic development in the rainiest place on Earth: Reconstructing the Shillong Plateau uplift history with in-situ cosmogenic 10Be. **Earth and Planetary Science Letters**, v. 483, 2018.

56. SACEK, V. *et al*. Numerical modeling of weathering, erosion, sedimentation, and uplift in a triple junction divergent margin. **Geochemistry, Geophysics, Geosystems**, v. 20, n. 5, 2019.

57. SANTOS, E. J.; MEDEIROS, V. C. Constraints from granitic plutonism on Proterozoic crustal growth of the Transverse Zone, Borborema Province, NE Brazil. **Revista Brasileira de Geociências**, v. 29, n. l, 1999.

58. SASSOLAS-SERRAYET, T.; CATTIN, R.; FERRY, M. The shape of watersheds. **Nature communications**, v. 9, n. 1, 2018.

59. SCHUMM, S. A. Evolution of drainage systems and slopes in badlands at Perth Amboy, New Jersey. **Geological Society of America Bulletin**, v. 67, n. 5, 1956.

60. SHAPIRO, S. S.; WILK, M. B. An analysis of variance test for normality (complete samples). **Biometrika**, v. 52, n. 3/4, p. 591-611, 1965.

61. SISKA, P. P. *et al*. Predicting ordinary kriging errors caused by surface roughness and dissectivity. **Earth Surface Processes and Landforms**, v. 30, n. 5, 2005.

62. SMALL, E. E.; ANDERSON, R. S. Pleistocene relief production in Laramide mountain ranges, western United States. **Geology**, v. 26, n. 2, p. 123-126, 1998.

63. STRAHLER, A. N. Hypsometric (area-altitude) analysis of erosional topography. **Geological Society of America Bulletin**, v. 63, n. 11, 1952.

64. SUMMERFIELD, M. A. **Global Geomorphology**. Essex: Longman Scientific and Technical, 1991.

65. TAVARES, B. A. C. **A participação da morfoestrutura na gênese da compartimentação geomorfológica do Gráben do Cariatá, Paraíba**. Tese (doutorado em Geografia). UFPE: Recife, 2010.

66. TAVARES, B. A. C. *et al*. Compartimentação geomorfológica e morfotectônica do Gráben do Cariatá, Paraíba, a partir de imageamento remoto. **Revista Brasileira de Geomorfologia**, v. 15, n. 4, 2014.

67. TINKLER, K. J.; WOHL, E. **Rivers over rock**. American Geophysical Union, 1998.

68. TURNER, J. P. et al. Thermal history of the Rio Muni (West Africa) – NE Brazil margins during continental breakup. **Earth and Planetary Science Letters**, v. 270, n. 3-4, 2008.

69. TWIDALE, C. R. On the origin of sediments in different structural settings. **Journal of Science**, v. 278, 1978.

70. TWIDALE, C. R.; BOURNE, J. A. Pediments as etch forms: implications for landscape evolution. **The Journal of Geology**, v. 121, n. 6, 2013a.

71. TWIDALE, C.; BOURNE, J. Do pediplains exist? Suggested criteria and examples. **Zeitschrift Für Geomorphologie**. 2013b.

72. VALERIANO, M. de M.; ROSSETTI, D.F. **Topodata**: seleção de coeficientes geoestatísticos para refinamento unificado de dados SRTM. São José dos Campos: INPE, 2010.

73. VAN SCHMUS, W. R. *et al*. Precambrian history of the Zona Transversal of the Borborema Province, NE Brazil: insights from Sm–Nd and U–Pb geochronology. **Journal of South American Earth Sciences**, v. 31, n. 2-3, 2011.

74. WHIPPLE, K. X. Bedrock rivers and the geomorphology of active orogens. **Annu. Rev. Earth Planet. Sci.**, v. 32, 2004.

75. WILLGOOSE, G.; HANCOCK, G. Revisiting the hypsometric curve as an indicator of form and process in transport-limited catchment. **Earth Surface Processes and Landforms**, v. 23, n. 7, 1998.

76. YAMAMOTO, J. K.; LANDIM, P. M. B. **Geoestatística**: conceitos e aplicações. São Paulo: Oficina de Textos, 2013.